Bioorganic & Medicinal Chemistry Letters 20 (2010) 4885–4891

Contents lists available at ScienceDirect

Bioorganic & Medicinal Chemistry Letters

journal homepage: www.elsevier.com/locate/bmcl

Enhanced selectivity profile of pyrazole-urea based DFG-out p38α inhibitors

Hu Liu [a,*], Cyrille Kuhn [a], Frederic Feru [a], Suzanne L. Jacques [b], Gayatri D. Deshmukh [b], Ping Ye [a], Glen R. Rennie [a], Theresa Johnson [a], Steven Kazmirski [c], Simon Low [c], Rocco Coli [b], Yuan-hua Ding [c], Alan C. Cheng [a], Haile Tecle [a], Jessie M. English [b], Robert Stanton [a], Joe C. Wu [b,*]

[a] Department of Chemistry, Cambridge South Laboratories, Pfizer Inc., 620 Memorial Drive, Cambridge, MA 02139, USA
[b] Department of Biochemistry, Cambridge South Laboratories, Pfizer Inc., 620 Memorial Drive, Cambridge, MA 02139, USA
[c] Department of Structural Biology, Cambridge South Laboratories, Pfizer Inc., 620 Memorial Drive, Cambridge, MA 02139, USA

ARTICLE INFO

Article history:
Received 11 April 2010
Revised 11 June 2010
Accepted 14 June 2010
Available online 17 June 2010

Keywords:
Kinase inhibitor
p38
Pyrazole-urea
DFG-out

ABSTRACT

By targeting an extended region of the conventional 'DFG-out' pocket of p38α, while minimizing interactions with the specificity pocket and eliminating interactions with the adenine binding site, we are able to design and synthesize a number of pyrazole-urea based DFG-out p38α inhibitors with good potencies, and excellent selectivity.

Mitogen-activated protein kinases (MAPKs) are important components of signal transduction pathways that mediate cell proliferation, differentiation, and death.[1] p38 is a critical member of this family and is important in enabling the production of pro-inflammatory cytokines such as TNF and IL-1.[2] Injectable biologic therapies that bind and inactivate TNF are effective treatments for rheumatoid arthritis and psoriasis.[3] Consequently, inhibition of p38 with a small molecule kinase inhibitor could provide an effective oral therapy for the chronic treatment of these autoimmune diseases. This belief is further evidenced by the fact that several p38α kinase inhibitors have reached clinical trials.[4]

Although ATP mimetics are still the mainstream platform for developing kinase inhibitors, wherein small molecules target the ATP pocket,[5] this approach has led to many recurring concerns/problems: (1) achieving selectivity among the >500 kinases in the genome; (2) selectivity for other proteins which use ATP as a substrate; (3) poor inhibitor pharmacokinetics (PK) properties, including solubility, and bioavailability. These problems have led to an increased interest in identifying novel protein kinase inhibitors whose potency is derived at least in part from interactions outside of the ATP binding pocket, referred to here as a nonclassical approach and 'nonclassical kinase inhibitors' (NCKIs).[6] Among the NCKIs, inhibitors that bind to the DFG-out conformations of kinases[7] have gained increasing attention from the pharmaceutical industry, largely due to the clinical and subsequent commercial success of DFG-out inhibitors such as imatinib[8] for cABL kinase (Novartis), and sorafenib[9] for Raf kinase (Bayer, Scheme 1). Among p38 inhibitors, a notable example is Boehringer Ingelheim's doramapimod (BIRB796, Scheme 1).[10] BIRB796 is a NCKI that binds to p38α in the DFG-out mode,[11] and was discontinued from further development in phase II. While the reason for BIRB796's failure in the clinic is not apparent from the literature, we suspect lack of selectivity might be culpable. We believe that p38 inhibitors with further enhanced margins of selectivity against other kinases would have improved safety margins and greater clinical tolerance for chronic treatment of autoimmune diseases.

The rationale for the current study arises from the observation that most of the known 'DFG-out' inhibitors, including Imatinib, Sorafenib and BIRB796, bind to their respective targets not only in the 'DFG-out' pocket made available by the movement of the phenylalanine residue in the conserved DFG segment of the kinase activation loop, but also within the ATP pocket and the adjacent kinase specificity pocket. The additional binding of these inhibitors with hinge residues in the adenine binding pocket is often required to achieve desired potencies. Although the 'DFG-out' inhibitors are known for improved selectivity profiles,[6] many of them do cross inhibit other kinases, especially when tested at high inhibitor concentration, such as 10 μM (Fig. 1).[12]

We speculated that inhibitors that bind primarily within the DFG-out pocket and minimally interact with the kinase specificity pocket, but lack direct interactions with the adenine binding site, might possess greater selectivity and improved safety margin. To-

* Corresponding authors. Tel.: +1 617 551 3302; fax: +1 617 551 3084 (H.L.); tel.: +1 617 995 2951 (J.C.W).
E-mail addresses: hu.liu@pfizer.com (H. Liu), joewu@aileronrx.com (J.C. Wu).

0960-894X/$ - see front matter © 2010 Elsevier Ltd. All rights reserved.
doi:10.1016/j.bmcl.2010.06.073

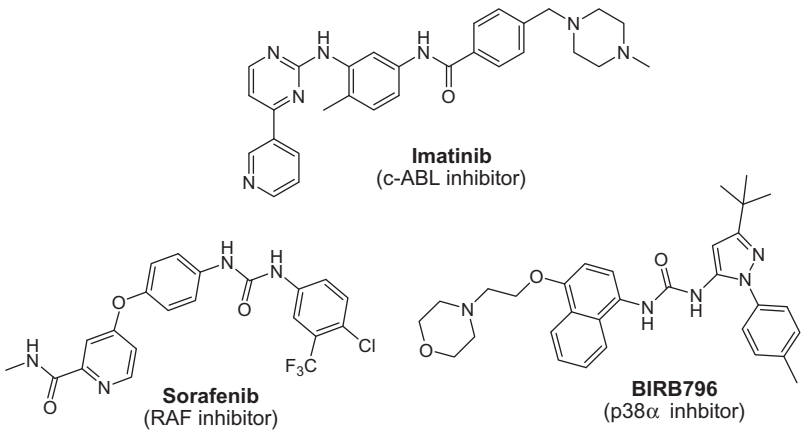

Scheme 1. Representative NCKIs that bind to the DFG-out conformations of kinases.

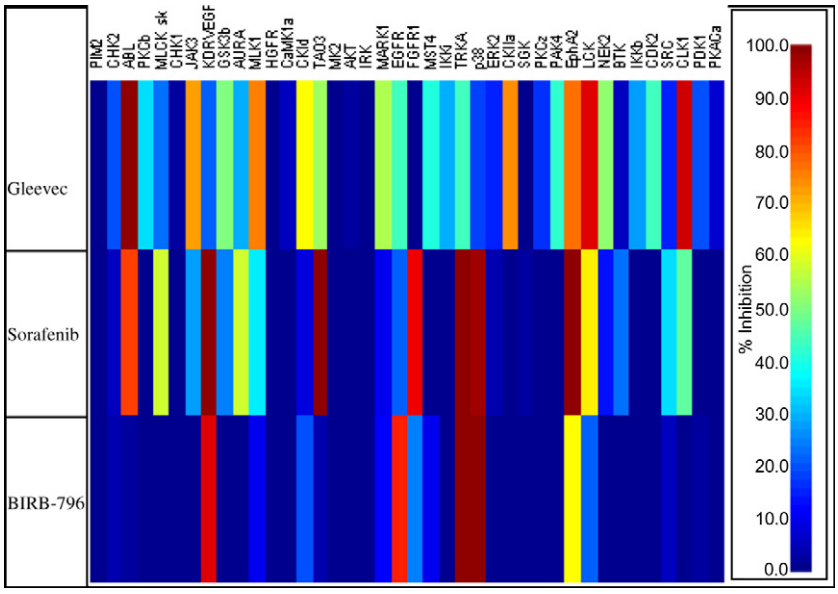

Figure 1. Selectivity profiles of imatinib, sorafenib and BIRB796 against a panel of 40 kinases at 10 μM.

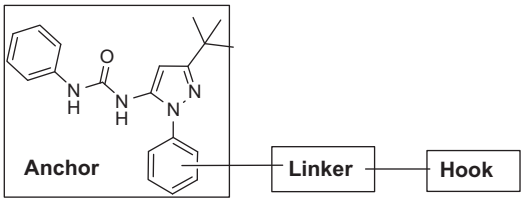

Scheme 2. Design of novel pyrazolyl-urea based p38α inhibitors.

ward that end, we designed novel pyrazolyl-urea based p38α inhibitors that contain a simple pyrazolyl-urea as the anchor, and additional linker and 'hook' moieties, wherein the 'hook' moiety contains a suitable combination of H-bond acceptors and donors (Scheme 2). While the simple pyrazolyl-urea anchor is expected to minimize interactions with the adenine binding site, the combined linker and 'hook' groups are expected to achieve desired potencies, improve selectivity, and serve as a handle for physical property modifications.

The synthesis of pyrazolyl-ureas **6** and **7**, with aminomethyl moieties suitable for further synthetic elaborations, is shown in Scheme 3. Diazotization of 3-aminobenzonitrile (**1**), followed by tin (II) chloride promoted reduction, and neutralization gave the free 3-hydrazinylbenzonitrile (**3**) in a 57% overall yield for three steps. Refluxing the nitrile **3** and 4,4-dimethyl-3-oxopentanenitrile in toluene resulted in the closure of the pyrazole ring to provide pyrazolyl-benzonitrile **4** in 50% yield. Treatment of **4** with the appropriate isocyanate afforded ureas **5a/5b** in acceptable yields. LAH reduction of the nitrile moieties in **5a/5b** gave the aminomethyl derivatives **6a/6b** in good yields. Pyrazolyl-phenylurea **6a** was further converted to its methylated derivative via reductive amination conditions in low yield (18%).

With pyrazolyl-phenylureas **6** and **7** in hand, we then turned our attention towards the synthesis of their amide derivatives **8** and **9** using standard coupling conditions (Table 1). Compounds **8** and **9** were evaluated in p38α cascade assays,[13] which provide a method to kinetically determine the binding of a compound to active or inactive p38α. In the active p38α cascade assay, compounds are first preincubated with active p38α before activity is determined by the addition of MK2 and its substrate. In the case of the unactive p38α cascade assay, compounds are preincubated with unactive p38α, followed by activation by MKK6 and then dilution into a MK2 and substrate mixture.

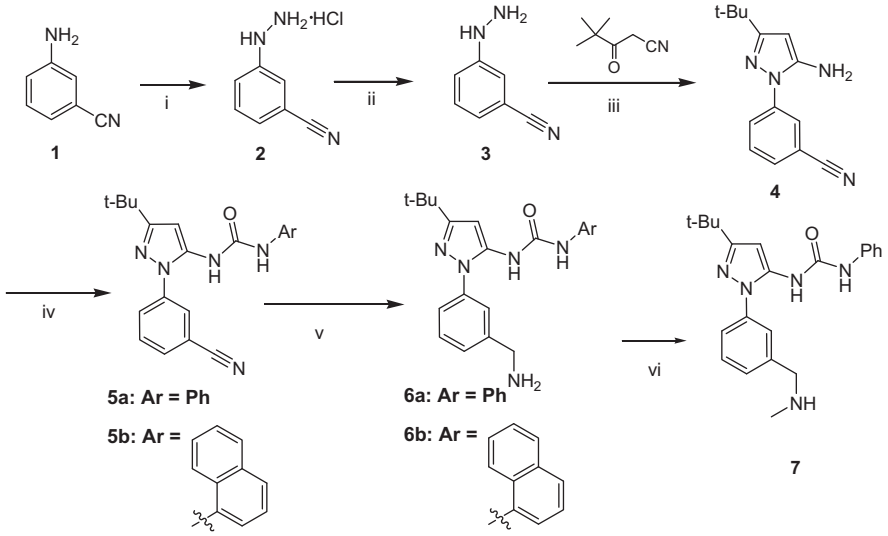

Scheme 3. Synthesis of pyrazolyl-3-phenylurea intermediates **6** and **7**. Reagents and conditions: (i) (a) $NaNO_2$, HCl; (b) $SnCl_2$, HCl, 78%; (ii) $NaHCO_3$, 73%; (iii) toluene, reflux, 50%; (iv) Ar–N=C=O, CH_2Cl_2, reflux, 50–60%; (v) $LiAlH_4$, THF, rt, 96–64%; (vi) (a) formaldehyde, toluene, 80 °C; (b) $NaBH_4$, rt, THF, 18%.

Table 1
Synthesis and evaluation **8**/**9** in p38α cascade assay

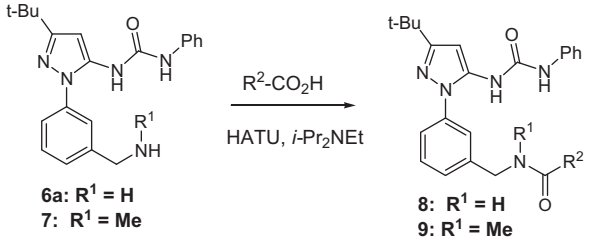

Entry	Compound	R^1	R^2	IC_{50} against unactive p38α (μM)[a]	IC_{50} against active p38α (μM)[a]
1	**6a**	H		2.85	>16.7
2	**8a**	H	$-CH_2NH_2$	0.176	2.3
3	**8b**	H	$-CH_2NH-C(O)-O-Me$	0.176	0.287
4	**8c**	H	$-CH_2NH-C(O)-H$	0.068	0.332
5	**8d**	H	$-CH_2NH-C(O)-CH_3$	0.006	0.034
6	**8e**	H	$-CH_2NH-C(O)-Ph$	0.169	0.441
7	**8f**	H	$-CH_2NH-C(O)$-3-pyridyl	0.051	0.205
8	**8g**	H	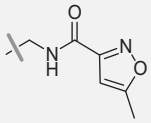	0.038	0.243
9	**8h**	H	$-CH_2NH-C(O)$-2-furanyl	0.018	0.088
10	**8i**	H	(*rac*)–CH(Me)–NH–C(O)–CH_3	0.168	0.48
11	**8j**	H	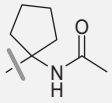	0.715	4.55
12	**8k**	H	$-CH_2NH-S(O)_2-CH_3$	0.108	0.649
13	**9a**	Me	$-CH_2NH-C(O)-CH_3$	0.211	1.6

[a] Average of three experiments with SD <15%.

As shown in Table 1, all the pyrazolyl-phenylurea derivatives tested in Table 1 show better potencies in the unactive p38α cascade assay, than in the active p38α cascade assay. This observation is in agreement with the assumption that the pyrazolyl-phenylureas **6a**, **8** and **9**, which are 'DFG-out' type inhibitors for p38α,[14] have better binding affinities towards unactive p38α versus its active form. For example, compound **6a** (Table 1, entry 1), which represents the pyrazolyl-phenylurea anchor, has an IC_{50} of 2.85 μM against unactive p38α, and an IC_{50} >16.7 μM against active p38α. Further elongation from the pyrazolyl-phenylurea anchor, such as in compound **8a** (Table 1, entry 2), results in a dramatically improved potency against both unactive and active p38α. Although a methyl carbamate moiety (**8b**, Table 1, entry 3) at the end of the chain does not improve the potencies further (IC_{50}'s of 0.176 μM and 0.287 μM against unactive and active p38α, respectively), the NH-Ac-glycine derivative **8d** (Table 1,entry 5) demonstrates

Table 2
Evaluation of **8l–8s** in p38α cascade assay

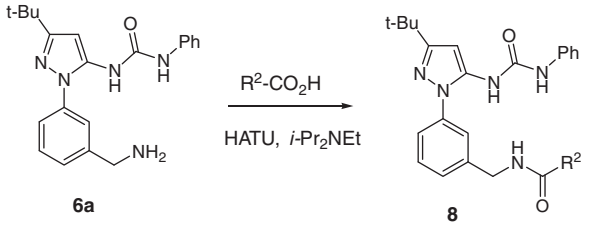

6a 8

Entry	Compound	R^2	IC_{50} against unactive p38α (μM)[a]	IC_{50} against active p38α (μM)[a]
1	**8d**	$-CH_2NH-C(O)-CH_3$	0.006	0.034
2	**8l**	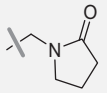	0.068	0.296
3	**8m**	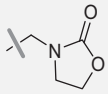	0.185	0.599
4	**8n**	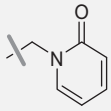	0.016	0.063
5	**8o**	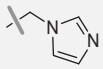	0.231	0.536
6	**8p**	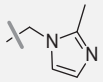	0.132	0.677
7	**8q**	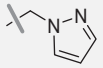	0.0488	0.135
8	**8r**	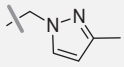	0.0279	0.201
9	**8s**	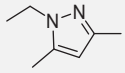	0.0782	0.331

[a] Average of three experiments with SD <15%.

excellent potencies against both unactive and active p38α (IC_{50}'s of 0.006 μM and 0.034 μM, respectively). Further examination around the NH-Ac-glycine side chain (Table 1, entries 6–11) revealed the following: (a) the acetyl amide 'hook' moiety could be replaced with other type of amides, such as small heteroaryl amides (e.g., Table 1, entries 8 and 9); (b) the α-position of the NH-Ac-glycine side chain has limited tolerance for lipophilic substitutions (e.g., Table 1, entries 10 and 11). It is also important to notice that changing the acetamide to methyl sulfonamide results in loss of potency (Table 1, entries 12 vs 5). Similarly, blocking the NH group immediately off the anchor with a methyl group (Table 1, entries 13 vs 5) also significantly diminishes potencies.

More detailed structure–activity relationship (SAR) studies around compound **8d** were carried out and the results summarized in Table 2. The presence of a H-bond acceptor in the 'hook' region is required for potency, yet the presence of a H-bond donor is much less essential (Table 2, entry 1 vs entries 2 and 4). For example, compound **8n** (Table 2, entry 4), wherein a pyridone moiety serves as the hydrogen bonding group in the 'hook' area, has an IC_{50} of 0.016 μM against unactive p38α, and an IC_{50} of 0.063 μM against active p38α. The spatial disposition of the H-bond acceptor is also crucial for potency. Indeed, pyrazole type hydrogen bonding groups (Table 2, entries 7–9) are more preferred over imidazole type hydrogen bonding groups (Table 2, entries 5 and 6).

Selectivity data for the NH-Ac derived pyrazolyl-phenylurea **8d** against a panel of 40 kinases at 10 μM is shown in Figure 2, and remarkable selectivity is observed. This result supports the key rationale for the design of these pyrazolyl-phenylureas, which is

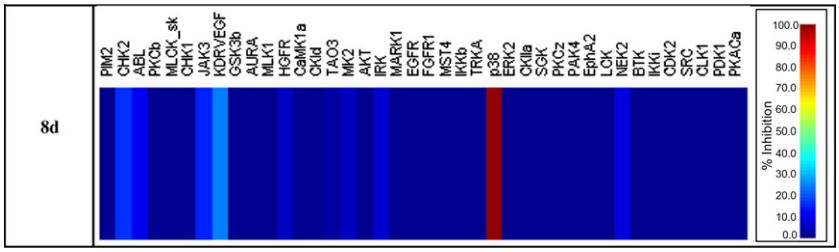

Figure 2. Selectivity profile of **8d** against a panel of 40 kinases at 10 μM.

Table 3
Evaluation of **8d**, **8n** and **8r** in in vitro ADME and safety assays

Entry	Compound	Solubility (turbidimetric, pH 6.5, phosphate buffer) (μM)[a]	PAMPA (Papp) (cm/s)	Human microsomal clearance (CLh) (mL/min/kg)	Dofetilide binding (% inhibition at 10 μm)	DDI-CYP inhibition (% inhibition at 3 μm)
1	**8d**	>200	7.38×10^{-6}	13.3	−11%	1A2 5% 2C9 0% 2D6 2% 3A4 0%
2	**8n**	50–150	12.9×10^{-6}	17.9	9%	1A2 4% 2C9 6% 2D6 21% 3A4 30%
3	**8r**	100–200	4.80×10^{-6}	18.6	3%	1A2 4% 2C9 5% 2D6 18% 3A4 26%

[a] Data are shown as the range of maximum kinetic solubility and minimum kinetic solubility.

that greater selectivity is possible from compounds that bind mainly within the DFG-out pocket, with no direct interaction with the adenine binding site, and minimized interactions with the kinase specificity pocket; and this potential is further realized by the right choices of linker and 'hook' moieties.

Some of the representative compounds from Tables 1 and 2 (**8d**, **8n** and **8r**) were further tested for their in vitro ADME and safety profiles, and the results are summarized in Table 3. Compound **8d** demonstrates an acceptable combination of solubility and permeability, as determined in the partial artificial membrane perme-

Table 4
Synthesis and evaluation of **11**/**12** in p38α cascade assay

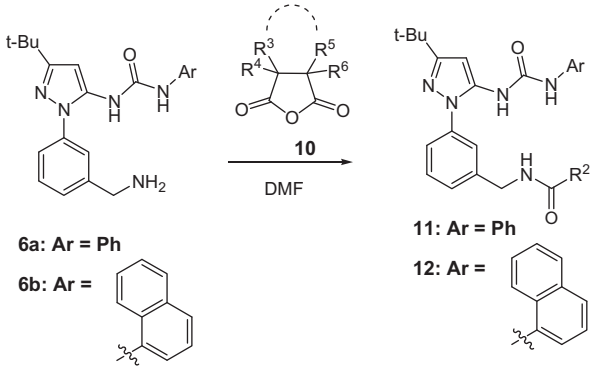

Entry	Compound	Ar	R^2	IC_{50} against unactive p38α (μM)[a]	IC_{50} against active p38α (μM)[a]
1	**11a**	Ph	$-CH_2CH_2-C(O)OH$	0.037	0.393
2	**11b**	Ph	$-CH_2C(Me)_2-C(O)OH$	0.039	3.68
3	**11c**	Ph	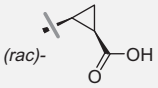	0.030	1.1
4	**11d**	Ph	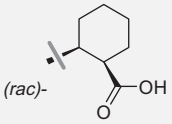	0.057	3.36
5	**11e**	Ph	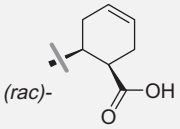	0.014	0.737
6	**12**	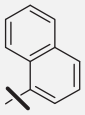	$-CH_2CH_2-C(O)OH$	0.005	0.006

[a] Average of three experiments with SD <15%.

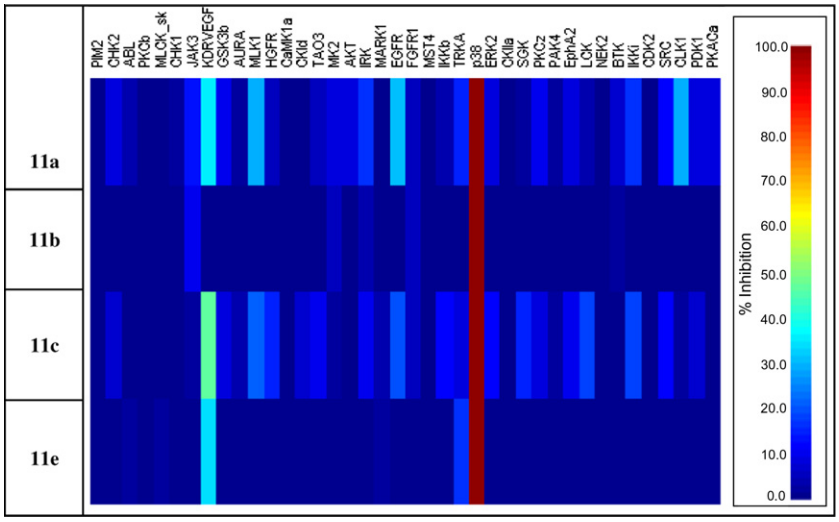

Figure 3. Selectivity profiles of **11a**, **11b**, **11c** and **11e** against a panel of 40 kinases at 10 μM.

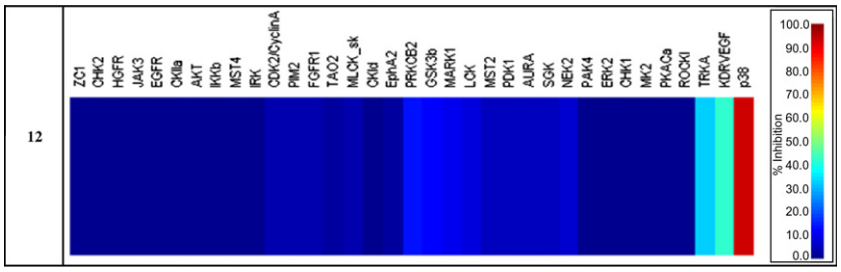

Figure 4. Selectivity profile of **12** against a panel of 35 kinases at 10 μM.

Table 5
Evaluation of **11a**, **11b**, **11c** and **11e** in in vitro ADME and safety assays

Entry	Compound	Solubility (turbidimetric, pH 6.5, phosphate buffer) (μM)[a]	PAMPA (Papp) (cm/s)	Human microsomal clearance (CLh) (mL/min/kg)	Dofetilide binding (% inhibition at 10 μm)	DDI-CYP inhibition (% inhibition at 3 μm)
1	**11a**	100–200	5.57×10^{-6}	<5.00	−2%	1A2 0% 2C9 0% 2D6 0% 3A4 0%
2	**11b**	>200	10.9×10^{-6}	7.23	−5%	1A2 17% 2C9 3% 2D6 0% 3A4 10%
3	**11c**	>200	4.94×10^{-6}	<5.28	−4%	1A2 0% 2C9 0% 2D6 0% 3A4 0%
4	**11e**	100–200	9.48×10^{-6}	10.5	−7%	1A2 10% 2C9 8% 2D6 6% 3A4 4%

[a] Data are shown as the range of maximum kinetic solubility and minimum kinetic solubility.

ation assay (PAMPA) (Table 3, entry 1). Furthermore, **8d** does not notably inhibit a cocktail of CYP P450 enzymes that consists of CYP1A2, 2C9, 2D6, 3A4, and does not interfere with dofetilide binding. However, all three evaluated compounds showed poor stability in human liver microsome assays, which we believe is at least partially caused by their high distribution coefficients at physiological pH (Log *D*).

As mentioned earlier, the combination of the linker and 'hook' moieties could also serve as a handle for physical property modifications. Toward that end, reacting the aminomethyl-pyrazolyl-ur-

eas **6** with cyclic anhydrides **10** (wherein R^3 and R^5 optionally forms a ring) in DMF provided pyrazolyl-phenylureas **11**/**12** with a carboxylic acid moiety as the 'hook' group. These compounds were evaluated in the p38α cascade assays (Table 4).

Compound **11a**, which has a flexible oxobutanoic acid side chain, has an IC_{50} of 0.037 μM against unactive p38α, and an IC_{50} of 0.393 μM against active p38α (Table 4, entry 1). Substitutions at the α-carbon of the acid moiety are also well tolerated (**11b**, Table 4, entry 2). More conformational restrained analogues, such as **11c** and **11d** (Table 4, entries 3 and 4), retained their inhibitory activity. On the other hand, cyclohex-3-enecarboxylic acid derivative **11e**, which has an unsaturated carbocycle (Table 4, entry 5), has slightly improved potency. Furthermore, it is interesting to notice that switching from a phenyl urea to a naphthyl urea resulted in **12**, which has an IC_{50} of 0.005 μM against unactive p38α, and an IC_{50} of 0.006 μM against active p38α (Table 4, entry 6). This likely is caused by an increased lipophilic occupancy in the specific binding area.

Some of the representative compounds from Table 4 were further tested for their selectivity against other kinases at 10 μM. As expected, remarkable selectivity is again observed for phenyl-pyrazole-urea acids **11a**, **11b**, **11c** and **11e** against a panel of 40 kinases (Fig. 3).

It is also interesting to notice that the naphthyl derivative **12**, which is highly potent against both unactive and active p38α (Table 4, entry 6), showed a similar selectivity profile at 10 μM against a slightly different panel of 35 kinases (Fig. 4).

Pyrazole-urea acids **11a**, **11b**, **11c** and **11e** were also tested in in vitro ADME and safety assays, and the results are summarized in Table 5. As expected, these acids show good solubility and improved stability in human liver microsome assays, when compared with neutral inhibitors, such as **8d** (Table 3, entry 1). On the other hand, these acids demonstrate a range of permeability, as determined in the PAMPA model, with introduction of lipophilic groups (**11e**, Table 5, entry 4) or steric hindrance around the acid moiety (**11b**, Table 5, entry 2) restoring the permeability to an excellent level. Furthermore, all compounds show clean profiles in the CYP P450 enzymes inhibition assays, and in the dofetilide binding assay.

In conclusion, we demonstrated that by simultaneously targeting the conventional 'DFG-out' pocket, and an extended region of p38α, we synthesized several pyrazole-urea based p38α inhibitors, which demonstrated good potencies and superior selectivity. These pyrazolyl-ureas differ from the well known 'DFG-out' type inhibitors, such as Imatinib, Sorafenib and BIRB796, in that they have no direct interactions with the adenine binding site, yet have selected linker and 'hook' moieties attached to the pyrazole-urea anchor, which allows them to achieve desired potencies, selectivity, and physical properties.

More thorough SAR studies on the 'hook' and linker regions, accompanied by fine tuning of the pyrazole-urea anchor are desired, as they will provide more insightful understanding of the pocket that interacts with the linker and 'hook' moiety, facilitate the development of a SBDD (structure-based drug design) platform, and hence delineate a path forward for applying this strategy to inhibitors for other kinases. These results will be published in the due course.

Acknowledgment

The authors thank Dr. Richard Nugent for helpful suggestions and discussions.

References and notes

1. (a) Rincon, M. *Curr. Opin. Immunol.* **2001**, *13*, 339; (b) Kuida, K.; Boucher, D. M. *J. Biol. Chem.* **2004**, *135*, 653.
2. (a) Johnson, G. L.; Lapadat, R. *Science* **2002**, *298*, 1911; (b) Schett, G.; Zwerina, J.; Firestein, G. *Ann. Rheum. Dis.* **2008**, *67*, 909; (c) Gaestel, M.; Mengel, A.; Bothe, U.; Asadullah, K. *Curr. Med. Chem.* **2007**, *14*, 2214.
3. (a) Sizova, L. *Br. J. Clin. Pharmacol.* **2008**, *66*, 173; (b) Lutt, J. R.; Deodhar, A. *Drugs* **2008**, *68*, 591.
4. (a) Pettus, L. H.; Wurz, R. P. *Curr. Top. Med. Chem.* **2008**, *8*, 1452; (b) Peifer, C.; Wagner, G.; Laufer, S. *Curr. Top. Med. Chem.* **2006**, *6*, 113; (c) Goldstein, D. M.; Gabriel, T. *Curr. Top. Med. Chem.* **2005**, *5*, 1017.
5. Gill, A. L.; Verdonk, M.; Boyle, R. G.; Taylor, R. *Curr. Top. Med. Chem.* **2007**, *7*, 1408.
6. Liao, J. J.-L. *J. Med. Chem.* **2007**, *50*, 409.
7. (a) Okram, B.; Nagle, A.; Adrian, F. J.; Lee, C.; Ren, P.; Wang, X.; Sim, T.; Xie, Y.; Wang, X.; Xia, G.; Spraggon, G.; Warmuth, M.; Liu, Y.; Gray, N. S. *Chem. Biol.* **2006**, *13*, 779; (b) Liu, Y.; Gray, N. S. *Nat. Chem. Biol.* **2006**, *2*, 358; (c) Sawa, M. *Mini-Rev. Med. Chem.* **2008**, *8*, 1291.
8. Mueller, B. A. *Curr. Pharm. Design* **2009**, *15*, 120.
9. Mendez-Sanchez, N.; Vasquez-Fernandez, F.; Zamora-Valdes, D.; Uribe, M. *Ann. Hepatol.* **2008**, *7*, 46.
10. (a) Regan, J.; Breitfelder, S.; Cirillo, P.; Gilmore, T.; Graham, A. G.; Hickey, E. R.; Klaus, B.; Madwed, J.; Moriak, M.; Moss, N.; Pargellis, C. A.; Pav, S.; Proto, A.; Swinamer, A.; Tong, L.; Torcellini, C. *J. Med. Chem.* **2002**, *45*, 2994; (b) Regan, J.; Capolino, A.; Cirillo, P. F.; Gilmore, T.; Graham, A. G.; Hickey, E.; Kroe, R. R.; Madwed, J.; Moriak, M.; Nelson, R.; Pargellis, C. A.; Swinamer, A.; Torcellini, C.; Tsang, M.; Moss, N. *J. Med. Chem.* **2003**, *46*, 4676; (c) Moss, N.; Breitfelder, S.; Betageri, R.; Cirillo, P. F.; Fadra, T.; Hickey, E. R.; Kirrane, T.; Kroe, R. R.; Madwed, J.; Nelson, R. M.; Pargellis, C. A.; Qian, K. C.; Regan, J.; Swinamer, A.; Torcellini, C. *Bioorg. Med. Chem. Lett.* **2007**, *17*, 4242.
11. Pargellis, C.; Tong, L.; Churchill, L.; Cirillo, P. F.; Gilmore, T.; Graham, A. G.; Grob, P. M.; Hickey, E. R.; Moss, N.; Pav, S.; Regan, J. *Nat. Struct. Biol.* **2002**, *9*, 268.
12. Card, A.; Caldwell, C.; Min, H.; Lokchander, B.; Xi, H.; Sciabola, S.; Kamath, A. V.; Clugston, S. L.; Tschantz, W. R.; Wang, L.; Moshinsky, D. J. *J. Biomol. Screen* **2009**, *141*, 31.
13. Tecle, H.; Feru, F.; Liu, H.; Kuhn, C.; Rennie, G.; Morris, M.; Shao, J.; Chang, A. C.; Gikunju, D.; Miret, J.; Coli, R.; Xi, S.; Clugston, S. L.; Low, S.; Kazmirski, S.; Ding, Y.-H.; Cao, Q.; Johnson, T. L.; Deshmukh, G. D.; DiNitto, J. P.; Wu, J. C.; English, J. M. *Chem. Biol. Drug Des.* **2009**, *74*, 547.
14. The p-38α co-crystals with this class of compounds are often partially resolved for the ligands. Nevertheless, based on some of the partially resolved structures, it is clear that these ureas bind to the 'DFG-out' conformation of the protein.